Spectral Analysis Using BayesWave for Characterizing Remnant Outcomes in Binary Neutron Star Mergers
Caltech LIGO SURF 2024, Final Report

Lana Alabbasi, Supervised by Isaac Legred and Katerina Chatziioannou
(Dated: September 29, 2024)

Neutron stars provide key insights into extreme stellar physics, with the detection of GW170817 marking the start of multimessenger astronomy by revealing both gravitational and electromagnetic signals. However, current gravitational wave detectors struggle to capture the postmerger phase, which holds crucial information about the remnant's characteristics and the nuclear equation of state (EoS). This research investigates the postmerger phase of binary neutron star (BNS) mergers using the morphology-agnostic BayesWave CPP algorithm, where we employed sine-Gaussian wavelets for adaptive signal reconstruction. By analyzing simulated signals of stiff and soft EoSs informed by numerical relativity at Cosmic Explorer (CE) sensitivity, we distinguished between long-lived neutron star remnants and those that promptly collapse into black holes. BayesWave CPP proved efficient in reconstructing the signals, accurately capturing the dominant and subdominant gravitational wave frequency modes at CE sensitivity. Additionally, in the promptly collapsing cases, we found that high-frequency oscillations identified in numerical simulations are associated with quasiradial stellar oscillations, rather than black hole ringdown quasinormal modes. Overall, this research highlights the effectiveness of BayesWave CPP for postmerger signal reconstruction and its potential to tackle the complex physics of BNS mergers and their remnants.

I. INTRODUCTION

Neutron stars offer a unique window into understanding the extreme physics of stellar structures. They serve as the densest mediums that can be directly observed across the sky, unlike black holes, which harbour no observable matter due to their immense gravity, hindering direct investigation of their medium properties. Neutron stars in binary systems provide a crucial outlook for precise mass measurements to understand their properties. In particular, gravitational-wave binaries allow for highly accurate mass determinations by analyzing the tidal deformability observed in the gravitational wave signal [1].

On August 17, 2017, the LIGO-Virgo collaboration observed a gravitational wave signal, GW170817, from the inspiral of two low-mass compact objects consistent with a binary neutron star (BNS) merger. This marked the first multimessenger detection of a gravitational wave signal accompanied by electromagnetic radiation [2].

The GW170817 detection, while advancing our understanding of BNS mergers, was not loud enough for the postmerger gravitational wave signal to be detected. The postmerger phase is characterized by dominant and subdominant frequency modes that encode information about the newly formed remnant as it settles into a stable configuration. Thus, further analyses of these modes are required as they can provide key insights into the remnant's characteristics and the equation of state (EoS) of the high-density matter.

The remnant outcomes of BNS mergers can be classified based on the type of the nuclear EoS governing the neutron star structure. The EoS is a relationship that describes the connection between outward pressure and density. For a stiffer EoS, for a given density, higher pressure would allow the neutron star to sustain a more massive structure with a larger radius. Such an EoS would support a long-lived neutron star remnant. On the other hand, a softer EoS exhibits a lower pressure, causing the neutron star to become more compact and therefore more subject to promptly collapsing into a black hole.

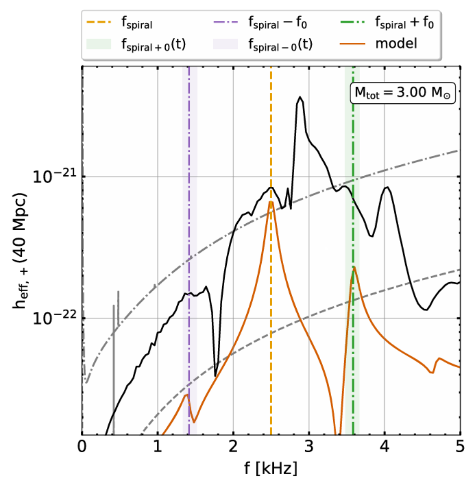

FIG. 1. The effective gravitational wave spectrum, $h_{eff}(f)$, reproduced from [3] for the postmerger phase of a long-lived remnant that is sustained through a stiffer EoS. The Vertical lines indicate the frequency peaks f_{peak}, f_{spiral}, f_{2+0}, and f_{2-0}. Shaded areas represent their frequency ranges. The dash-dotted curves denote the sensitivity levels of Advanced LIGO and the Einstein Telescope, respectively.

Looking at the spectral features of the effective spectrum of BNS mergers can give crucial insights into the evolution and potential remnant outcome of the binary. For Stiffer EoSs, which exhibit characteristics that align with the sustained presence of a neutron star, it can be

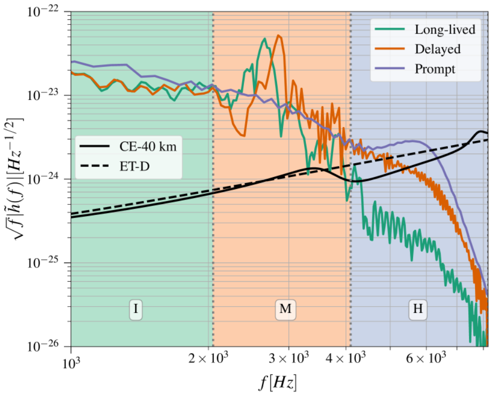

FIG. 2. Strain profiles for three BNS mergers at 100 Mpc reproduced from [4] revealing distinct remnant types. The sensitivity curves of two proposed next-generation observatories are depicted with solid and dashed black lines. The prompt collapse remnants linked to a softer EoS display a prominent peak near the fundamental quasinormal mode of the resulting black hole. The delayed collapse case which also corresponds to a softer EoS, shows excess power at these frequencies.

seen from Figure 1 that the frequencies of the gravitational wave signal can be well defined. It exhibits a dominant peak frequency that when varying over time can indicate the remnant's evolution. This peak corresponds to a linear feature, f_2 or f_{peak}, driven by quadrupolar oscillations. It is important to distinguish it from other potential contributors such as pressure and gravity modes, which are caused by different restoring forces [3]. Subdominant frequency modes include a quasiradial symmetric oscillation, f_0, which does not radiate gravitational waves. Therefore, even if oscillations in this mode are significant, they cannot be observed in the gravitational wave signal. Additional subdominant modes that do emit gravitational waves include the quasilinear features of f_{2+0} and f_{2-0}, which arise from couplings between quadrupolar and quasiradial oscillations, and a fully nonlinear feature, f_{spiral}, which corresponds to a transient spiral deformation.

For Softer EoSs which tend to promptly collapse, Figure 2 suggests less defined spectral features [4]. Such features could be interpreted to have frequency modes associated with an immediate transition to frequencies associated with a prompt collapse or a combination of black hole ringdown quasinormal modes (QNMs). This leads to a classification scheme of the postmerger gravitational wave emission depending on the nuclear EoS and the mass of the binary [5]. The relationship between the peak frequency and secondary frequencies, as well as the features observed in the spectrum between them, can offer insights into the remnant's lifespan and its potential evolution towards black hole formation.

II. MOTIVATIONS

This research project aimed to investigate the influence of the EoS governing high-density nuclear matter on the remnants of BNS mergers. Specifically, we sought to categorize long-lived neutron stars from those that ultimately collapse into black holes. To achieve this, we focused on the ringdown phase of the merger through analyzing the underlying physics to distinguish between black hole and neutron star collapse signatures.

It is generally understood that the dominant and subdominant frequency modes can be well identified theoretically in simulations for a long-lived remnant. However, it is not necessarily clear if future detectors like CE will be able to distinguish these modes in postmerger. Additionally, for the promptly collapsing case, it is uncertain whether they are QNMs or modes associated with the collapse of the star, such as the quadrupolar with quasiradial coupling mode, f_{2+0}. This uncertainty presents a significant motivation for our work. By studying the spectral features of the ringdown phase, we aim to better understand the physical distinctions between black holes and neutron star collapse, the significance of spectral frequency "bumps," and the information encoded in the gap between them. This will ultimately contribute to refining current methods for distinguishing remnant types and the remnant outcomes of BNS mergers based on the spectral features of the signals.

Another objective was to address the current limitations of gravitational wave detectors in capturing the postmerger phase of BNS mergers. Given these limitations, we sought to reconstruct the effective spectra of these remnants to assess the feasibility of future detectors with enhanced sensitivity in detecting and characterizing them. This data-driven approach would provide valuable insights into the feasibility of using gravitational wave observations, particularly for future detectors, to distinguish between black hole and neutron star collapse signatures and the properties of the high-density nuclear matter.

III. METHODS

Due to the inherent complexity of the postmerger signal, our analysis utilized the morphology-agnostic data analysis algorithm BayesWave to examine the frequencies and amplitudes of these modes. BayesWave is a data-driven algorithm that employs wavelets for signal reconstruction. In this project, we chose sine-Gaussian wavelets for their flexibility in reconstructing the postmerger signal from raw gravitational wave data. We specifically used BayesWave CPP, a newer and more efficient update of BayesWave, which is well-suited for diagnosing potential issues and delivering robust results [6].

A distinguishing feature of this analysis is its model-agnostic approach. Unlike studies that rely on specific waveform models, this research allows for arbitrary wavelet shapes, providing greater flexibility in capturing the complex dynamics of binary neutron star mergers. By replacing predetermined waveform models and priors, this analysis ensures that the data in the form of gravitational wave strain, remains independent and unconstrained by theoretical assumptions. This agnostic framework enables the sine-Gaussian wavelets to adapt freely to the observed signal, without being restricted to specific frequency relationships or configurations. Consequently, this method demonstrates its robustness in fitting a wide range of potential gravitational waveforms.

In the frequency domain, the peak's width exhibits an inverse relationship with the corresponding mode's duration. Therefore, short-lived modes have broad peaks, potentially leading to challenges in the analysis for their identification and separation from other components within the spectrum.

Since BNS mergers are rare events presenting consequent limitations in observational data, Bayesian statistics offer a powerful approach to address this limitation. We employ Bayesian inference to reconstruct the signal parameters, such as frequencies and amplitudes of the overlapping modes from the observed gravitational wave data. Unlike traditional frequentist methods, Bayesian inference allows us to incorporate prior knowledge about the system. The components utilized for the analysis are the same ones needed to work out Bayes theorem. Its mathematical framework enables us to quantify the targeted probability, which is defined as

$$P(h|d) = \frac{P(d|h) \cdot P(h)}{P(d)} \tag{1}$$

where we aimed to estimate the posterior of the signal parameters, $P(h|d)$, to compare the reconstructed signal parameters from its distribution to numerical relativity simulations at the Cosmic Explorer (CE) sensitivity. The likelihood function, $P(d|h)$, represents the probability of obtaining the observed data, d, given the specific signal parameters, h [7] . Additionally, the evidence, $P(d)$, serves as a normalization factor. By applying Bayes' theorem, we can invert this likelihood to estimate the posterior probability of the signal parameters given the data. To ensure a flexible and comprehensive reconstruction, we adopt a broad prior distribution for the signal parameters. In our case, sine-Gaussian wavelets serve as the prior model. The likelihood function is calculated using a simulated signal and the detector's sensitivity model.

To simulate the conditions expected in the next-generation CE observatory, the injected signals were designed with a prior incorporating realistic noise characteristics. The longer arms of the detector, compared to LIGO's 4 km, will enhance its sensitivity. This is expected to enable the detection of BNS postmerger events with precision. For our simulations, we used the 20 km CE model to provide an estimate of its potential performance.

Figure 3 visually represents the Bayesian inference

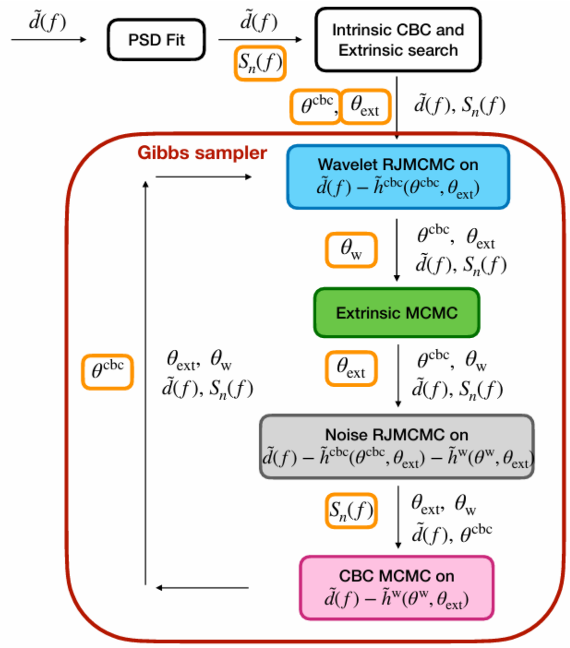

FIG. 3. A diagram reproduced from [6] showcasing the workflow of BayesWave. It involves data preprocessing, initial parameter estimation, and iterative updates using the blocked Gibbs sampler, which includes four independent samplers for wavelet, extrinsic, noise, and CBC parameters. When the Gibbs sampler is initialized, the independent samplers, wavelet RJMCMC, extrinsic MCMC, noise RJMCMC, and CBC MCMC iteratively update the corresponding parameters, refining the signal reconstruction.

workflow implemented in BayesWave, showcasing the way that the algorithm iteratively updates parameters that are related to wavelet modelling, extrinsic parameters, noise modelling, and the BNS merger parameters, also referred to as Compact Binary Coalescence (CBC). Therefore, implementing sine-Gaussian wavelets through BayesWave for signal reconstruction offers a refined opportunity to delve deeper into the complexities of the postmerger phase, which will provide a better understanding of the physical processes governing the remnants of BNS mergers.

IV. RESULTS

In this section, we present the outcomes of our comparative analysis of potential BNS merger remnants. Our investigation focuses on two primary models, which are long-lived remnants that are supported by a stiff EoS and promptly collapsing remnants, which result from a softer EoS. We explore the gravitational wave signatures produced by these distinct scenarios and assess the capabilities of BayesWave CPP in reconstructing such signals.

A. Long-lived and Prompt Collapse Models

A comparison between the two main types of potential BNS merger remnants was shown. For the long-lived stiff EoS model, it exhibits characteristics that align with the sustained presence of an oscillating neutron star. Therefore, a good analytic model for demonstrating such behaviour would be the exponentially damped sinusoids model where the peak frequency, f_{peak}, is changing while assuming all other frequencies of the model to be constant in time, the model is as follows

$$\begin{aligned} h_{+}(t) = A_{\text{peak}}\, e^{\left(-\frac{t}{\tau_{\text{peak}}}\right)} \cdot \sin(\phi_{\text{peak}}(t)) \\ + A_{spiral}\, e^{\left(-\frac{t}{\tau_{\text{spiral}}}\right)} \cdot \sin\left(2\pi f_{spiral} \cdot t + \phi_{spiral}\right) \\ + A_{2-0}\, e^{\left(-\frac{t}{\tau_{2-0}}\right)} \cdot \sin\left(2\pi f_{2-0} \cdot t + \phi_{2-0}\right) \\ + A_{2+0}\, e^{\left(-\frac{t}{\tau_{2+0}}\right)} \cdot \sin\left(2\pi f_{2+0} \cdot t + \phi_{2+0}\right) \end{aligned} \tag{2}$$

where the f_{peak} component's phase $\phi_{\text{peak}}(t)$ is

$$\phi_{\text{peak}}(t) = \begin{cases} 2\pi\left(f_{\text{peak},0} + \frac{\zeta_{\text{drift}}}{2} t\right) t + \phi_{\text{peak}}, & \text{for } t \leq t_* \\ 2\pi f_{\text{peak}}(t_*)(t - t_*) + \phi_{\text{peak}}(t_*). & \text{for } t > t_* \end{cases} \tag{3}$$

where ζ_{drift} is the rate at which f_{peak} of the gravitational wave signal changes as the remnant evolves, and t_* is the time at which the change of f_{peak} becomes constant. For this work, to show the change in the strain as a function of time showcasing the spectra of a long-lived neutron star remnant, all the dominant and subdominant frequency modes were set to be in kHz, $t_* = 0.2$ ms, $\zeta_{\text{drift}} = 0.5$ for a positively increasing rate of change of f_{peak}, and the $\phi_{\text{peak}}(t)$ is assumed to be equal to zero for simplification.

The promptly collapsing model that results from a softer EoS exhibits features that immediately transition to frequencies associated with a black hole ringdown. The equation for the ringdown signal, which is expressed as a complex exponential function models the ringdown phase of gravitational waves emitted by a black hole after the merger. The equation is as follows

$$h^R(t) = h_+^R(t) - i h_\times^R(t) = \sum_{lmn} A_{lmn} e^{-i[\omega_{lmn}(t-t_0) - \phi_{lmn}]} \tag{4}$$

where $t \geq t_0$ and A_{lmn} represents the amplitude, Φ_{lmn} to be the phase, and t_0 to be the start time of the ringdown.

To visually compare the two distinct models, we plotted the SXS0305 simulation, representing the ringdown waveform of the first gravitational wave detection, GW150914, against the damped sinusoids model. The comparison was made by scaling the amplitudes so they are the same at the start, with both models adjusted to match the amplitude of a BNS postmerger, as illustrated in Figure 4.

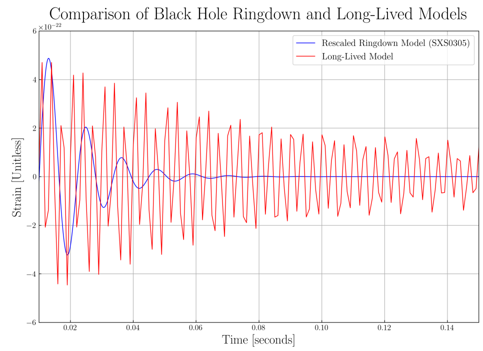

FIG. 4. Comparison of ringdown and damped sinusoids models. Both models are plotted at a BNS postmerger amplitude. The blue waveform represents the SXS0305 simulation of the ringdown from the first gravitational wave detection, GW150914. The red waveform illustrates the damped sinusoids model typical of a long-lived neutron star remnant. The comparison shows that the ringdown signal decays more rapidly than the damped sinusoids, indicating a quicker transition to a black hole in the ringdown scenario.

B. Signal Reconstructions Using BayesWave CPP

To assess the ability of BayesWave CPP to reconstruct the postmerger signals from BNS mergers, a series of simulation injections were conducted. These injections were inferred by numerical relativity simulations and were injected into BayesWave to incorporate realistic noise characteristics, using the 20 km CE model amplitude spectral density (ASD) up to 8 kHz. Additionally, other priors, such as an event distance of 40 Mpc, similar to the first BNS merger detected, GW170817, alongside a maximum frequency of 4000 Hz and the extrinsic parameters were fixed to the injected values.

To reconstruct the signals, BayesWave first converted the simulated data for the injected signal into a form that could be processed for our analysis. Then, Markov Chain Monte Carlo (MCMC) sampling was employed within the BayesWave main module to construct the posterior distribution, which represents the reconstructed signal. The MCMC sampling process iteratively updates parameters related to the sine-Gaussian wavelet modeling, the extrinsic parameters, the noise model, and the parameters of the merger.

Finally, BayesWave post was executed to generate plots comparing the injections to the reconstructions and to perform a diagnostic review. Reconstructions were conducted for two distinct EoSs, DD2, a stiff EoS that supports long-lived remnants, and MPA1, a softer EoS

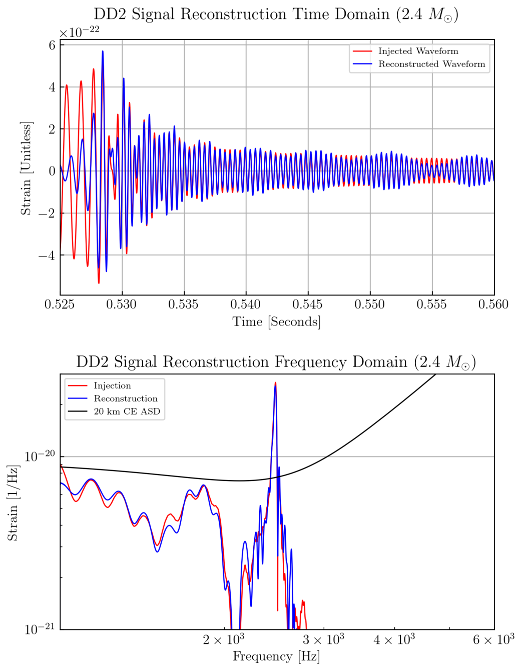

FIG. 5. Time and frequency domains signal injections in red, and reconstructions in blue, for the stiff DD2 EoS, a delayed collapse simulation with a total mass of 2.4 $M_\odot$. The results demonstrate that BayesWave CPP effectively reconstructs the injected signals at CE sensitivity, particularly for the frequency modes associated with a long-lived neutron star remnant.

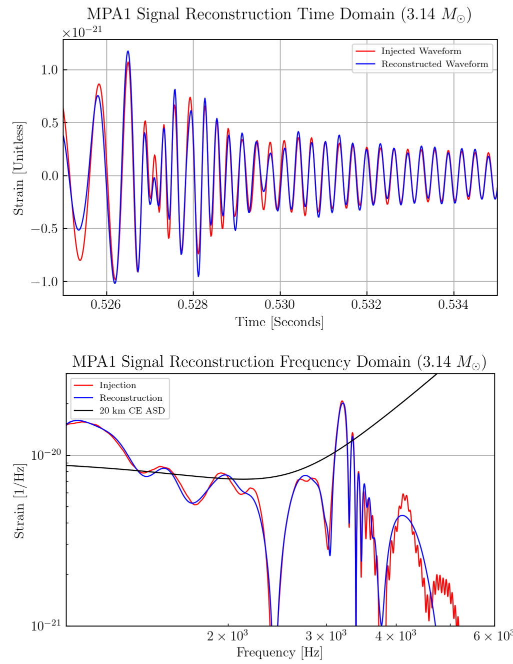

FIG. 6. Time and frequency domains signal injections in red, and reconstructions in blue, for the softer MPA1 EoS, a simulation reaching prompt collapse with a total mass of 3.14 $M_\odot$. The results demonstrate that BayesWave CPP effectively reconstructs the injected signals at CE sensitivity, particularly for the frequency modes where the remnant is substantially close to a prompt collapse.

leading to promptly collapsing remnants for higher total masses. A maximum of 14 wavelets was used in the BayesWave runs to ensure computational efficiency while maintaining adequate signal representation.

To achieve a systematic approach to comparing the outcomes of the runs, the mass ratio was constant, while varying the total mass as it is the variable that primarily controls whether a particular configuration will collapse into a black hole or not. The DD2 and the MPA1 EoS reconstructions in the time and frequency domains are shown in Figures 5 and 6. The results demonstrate that BayesWave CPP effectively reconstructs the injected signals at CE sensitivity. This suggests that the software is well-suited for analyzing data from future next-generation gravitational wave detectors.

Multiple things can be understood about the peak and secondary frequency modes by looking at the varying behaviour of the modes for the simulations. Firstly, the higher the total mass, the harder it becomes to identify f_{peak} as other secondary frequency modes become more excited. Secondly, since the DD2 simulation sustains a long-lived remnant, the decay time of the secondary modes takes approximately 5-6 milliseconds.

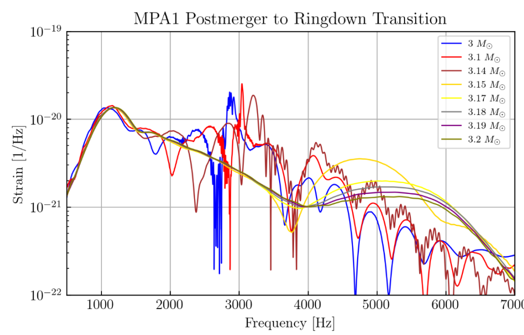

FIG. 7. A series of MPA1 EoS simulations reveal a critical threshold for prompt collapse, with a noticeable change in behaviour occurring around the 3.15 $M_\odot$ simulation in orange. This means that BNS systems with total masses that exceed this threshold are likely to undergo a rapid collapse directly into a black hole.

C. Identifying QNMs for Prompt Collapse

As shown in Figure 7, the MPA1 EoS simulations led to a prompt collapse transition at a higher total mass at approximately 3.15 $M_\odot$. Consequently, all simulations with higher masses were expected to undergo a ringdown phase. To estimate the ringdown frequencies for these promptly collapsing simulations, we analyzed the black

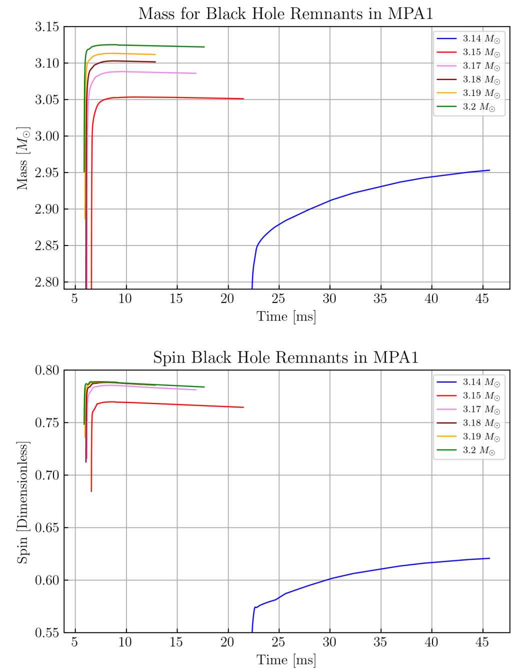

FIG. 8. The evolution of remnant black hole spin and mass with time for promptly collapsing MPA1 simulations is shown, starting from the 3.14 $M_\odot$ configuration in blue. This simulation stands out as the last to produce a long-lived remnant before transitioning to a black hole. The mass plot reveals a correlation between the remnant's final mass and the collapse time, with lower-mass remnants tending to collapse later. The spin plot shows that prompt collapse simulations typically result in black holes with spins of approximately 0.78.

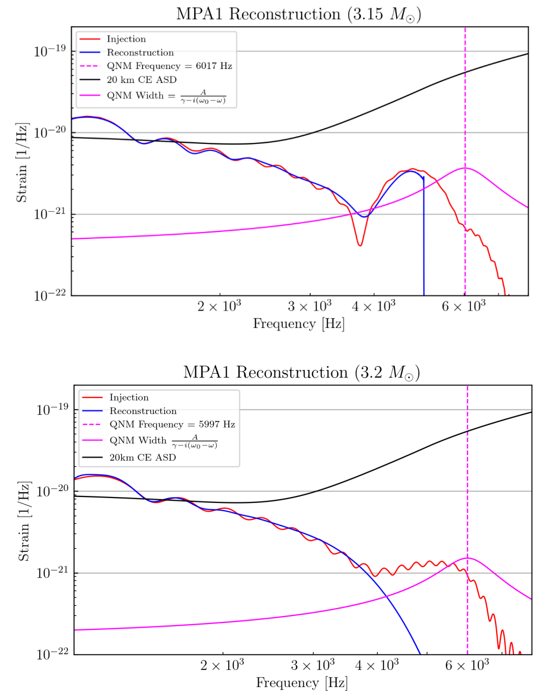

FIG. 9. The plots illustrate the injected signals in red, and the reconstructions in blue, for the promptly collapsing 3.15 $M_\odot$ and 3.2 $M_\odot$ MPA1 simulations. The dashed pink lines represent the calculated fundamental QNM frequencies of 6017 Hz and 5997 Hz, respectively, along with their corresponding Lorentzian distributions. Despite the presence of a prominent bump in the reconstructed waveforms, the simulations did not show a clear alignment with the predicted QNM distributions. This suggests that the bump might instead be associated with the f_{2+0} mode.

hole remnant spin and mass data. Figure 8 illustrates the evolution of spin and mass with time, starting from the 3.14 $M_\odot$ simulation.

Analysis of the mass plot reveals a correlation between the mass of the black hole remnant and the collapse time, where the remnants lower in mass tend to collapse later. For the spin plot, the prompt collapse simulations have spins of nearly 0.78. While typical spin values for black hole mergers are around 0.7, BNS remnants often have higher spins, approximately at 0.78. This suggests that the type of the merging objects, black holes or neutron stars, influences the final spin of the remnant object. As highlighted in both plots, the 3.14 $M_\odot$ simulation stands out as the last simulation to produce a long-lived remnant before transitioning to a black hole.

To calculate the fundamental QNM frequency tone of the ringdown, which corresponds to the simplest and lowest frequency oscillation of the black hole and the first overtone of the gravitational wave signal, we used the following equation

$$frequency = \frac{\omega}{2\pi M_{BH}} \frac{GM_\odot}{c^3} \tag{5}$$

where ω is the real part of the angular frequency of the fundamental QNM tone and M_{BH} is the mass of the black hole remnant.

To compare the calculated QNM frequency with the spectral features of the injected and reconstructed signals, we first determine it as a Lorentzian distribution. It included the amplitude, the real and the imaginary parts of the fundamental tone, as defined by the following equation

$$QNM = \frac{A}{\gamma - i(\omega_0 - \omega)} \tag{6}$$

The QNM frequencies and distributions were plotted for all the promptly collapsing reconstructions of the MPA1 EoS. As shown in Figure 9, initially, the QNM distribution appears to be close to the bump in the reconstruction, suggesting a potential overlap and confirming the feasibility of detecting QNMs from BNS mergers. However, since none of the simulations resulted in these two bumps aligning, it is likely that the bump reconstructed by BayesWave at CE sensitivity does not correspond to a QNM. Instead, it might represent the f_{2+0} mode, which typically appears at higher frequencies in the spectral plot.

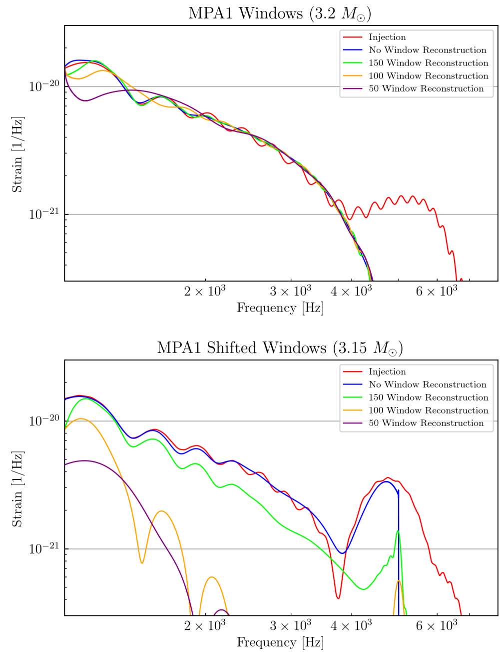

FIG. 10. The plots compare Tukey windows with varying sizes, 150, 100, and 50, applied to the 3.2 $M_\odot$ simulation, shown in green, orange, and purple, respectively, against the injection in red, and the unwindowed reconstruction in blue. In the 3.15 $M_\odot$ simulation, negative Tukey sizes were also used to detect any power from the ringdown phase. Both plots indicate that windowing had minimal effect on reconstructing the high-frequency bump or recovering the ringdown power.

This finding indicates that the f_{2+0} mode is well-detected at CE sensitivity levels, which is a substantial part of the postmerger when the configuration is near to collapse. The observed widening and shift of the bump to higher frequencies align with the expected behaviour of the f_{2+0} mode as the density increases for the same EoS.

D. Windowing the Reconstructions

To facilitate a more comprehensive analysis of postmerger waveforms, it is often beneficial to examine them in the frequency domain. This approach allows for a clearer identification of the characteristic features, such as the peak and secondary frequency modes, leading to a more coherent interpretation of the data.

When converting signals from the time domain to the frequency domain using the Fourier transform, the choice of the windowing function is important. This ensures that the observed frequency modes and their evolution represent the postmerger phase solely of the simulated signal to provide a more accurate and focused analysis.

To investigate the impact of windowing on the reconstruction of the high-frequency bump, Tukey windows with varying sizes of 150, 100, and 50 data points were applied to the 3.2 $M_\odot$ simulation. The numerical relativity simulations have a duration of 1 second with a sampling rate of 16,383 Hz. A Tukey window with a size of 50 data points spans approximately 3.05 milliseconds around the peak of the signal, while a size of 100 covers 6.1 milliseconds, and 150 covers 9.15 milliseconds. These windows help smooth out the edges of the signal and reduce discontinuities, therefore mitigating the Gibbs phenomenon, which causes oscillations and ripples near sharp transitions in the reconstructed signals. Despite this, as shown in Figure 10, windowing did not significantly improve the reconstruction of the high-frequency bump in the case of the MPA1 promptly collapsing simulations.

To further explore the potential contribution of the ringdown to the observed signal, Tukey windows with negative sizes were also employed. This approach effectively shifts the window in time, allowing for the identification of any power originating from the ringdown phase. However, the results indicate that the ringdown does not contribute substantially to the signal, even when using negative windowing.

In the 3.15 $M_\odot$ simulation, the ringdown was already not well modelled without any windowing, suggesting that windowing alone may not be sufficient to recover the ringdown power in these simulations. This highlights the need for more sophisticated techniques to accurately capture the ringdown signal in BNS mergers.

V. CONCLUSIONS

This research project has demonstrated the effectiveness of BayesWave CPP in reconstructing the numerically simulated postmerger gravitational wave signals from BNS mergers at the sensitivity level of the future detector, CE. Through a series of simulations, we have successfully inferred the key features of both long-lived and promptly collapsing remnants.

For long-lived remnants, supported by the stiff DD2 EoS, the reconstructed signals demonstrated characteristics consistent with a sustained oscillating neutron star. The damped sinusoids model, with its evolving peak frequency and constant secondary frequencies, provided a suitable representation of these signals. Conversely, the promptly collapsing remnants that resulted from the softer nature of the MPA1 EoS at higher total masses, transition directly to frequencies associated with black hole ringdown. The ringdown signal, expressed as a complex exponential function, accurately captures this behaviour.

A significant finding of this project is the detection of the f_{2+0} mode at the sensitivity level of the CE 20 km model, particularly near the collapse phase of the postmerger. This observation suggests that the f_{2+0} mode is a promising candidate for distinguishing between black hole and neutron star remnants. However, our analysis did not provide clear evidence for the detection of QNMs at CE sensitivity, and the bump observed in the reconstructions could potentially be attributed to the f_{2+0} mode rather than a QNM.

Furthermore, we explored the impact of windowing techniques on the reconstruction of the high-frequency bump in the promptly collapsing simulations. Our results indicate that windowing alone is not sufficient to recover the ringdown power in these cases, suggesting the need for more advanced methods to accurately capture the ringdown signal. In summary, this research has provided new insights into the capabilities of BayesWave CPP for postmerger signal reconstruction and its promising potential for gravitational wave observations to distinguish between black hole and neutron star remnants in BNS mergers.

VI. FUTURE PROSPECTS

Expanding the scope of the current analysis, to further enhance the capabilities of BayesWave CPP for postmerger signal reconstruction, several avenues can be explored. Considering the potential limitations of the sine-Gaussian wavelet model, particularly for the demonstrated envelope shape in the reconstructions, exploring alternative wavelets could provide a more suited model for similar analyses. The damped sinusoids model may serve as a good wavelet model for a smoother reconstruction. While possessing desirable properties, the damped sinusoids model would require careful windowing to mitigate the Gibbs phenomenon in the Fourier transform to avoid oscillations and ripples near sharp transitions. By investigating various wavelet models, we can identify those that better capture the evolving nature of postmerger signals and enhance the overall accuracy of the reconstruction.

Furthermore, increasing the maximum number of wavelets used in BayesWave could potentially improve the reconstruction quality. While this may increase computational costs, it could lead to more precise representations of the postmerger signal, especially for complex waveforms.

Another important consideration is testing the capabilities of BayesWave to reconstruct the signals at the 40 km CE model instead of the 20 km one. Since CE is frequency-dependent due to the phase shift of the passing gravitational waves, introducing a frequency shift in the data handed to BayesWave would be necessary to achieve accurate results.

Finally, extending the analysis to include a wider range of EoSs would provide a more comprehensive understanding of the diversity of BNS merger remnants and their associated gravitational wave signatures. By exploring different EoSs, we can identify potential correlations between them and the characteristics of the reconstructed signals, further refining our understanding of their underlying physics.

VII. ACKNOWLEDGEMENT

I would like to express my sincere gratitude to my mentors, Isaac Legred and Katerina Chatziioannou, for their invaluable guidance and support throughout this research project. Additionally, I am deeply grateful to Alan Weinstein and Jonnah Kanner for their exceptional management of the LIGO SURF program. Furthermore, I would like to thank the California Institute of Technology Student-Faculty Programs and the LIGO Scientific Collaboration for providing me with the opportunity to conduct this research, and the National Science Foundation for their funding and support for the LIGO Lab.

[1] A. Bauswein, H. T. Janka, K. Hebeler, and A. Schwenk. Equation-of-state dependence of the gravitational-wave signal from the ring-down phase of neutron-star mergers. *Phys. Rev. D*, 86:063001, 2012.

[2] B. P. Abbott et al. GW170817: Observation of Gravitational Waves from a Binary Neutron Star Inspiral. *Phys. Rev. Lett.*, 119(16):161101, 2017.

[3] Theodoros Soultanis, Andreas Bauswein, and Nikolaos Stergioulas. Analytic models of the spectral properties of gravitational waves from neutron star merger remnants. *Phys. Rev. D*, 105(4):043020, 2022.

[4] Arnab Dhani, David Radice, Jan Schütte-Engel, Susan Gardner, Bangalore Sathyaprakash, Domenico Logoteta, Albino Perego, and Rahul Kashyap. Prospects for direct detection of black hole formation in neutron star mergers with next-generation gravitational-wave detectors. *Phys. Rev. D*, 109(4):044071, 2024.

[5] James Alexander Clark, Andreas Bauswein, Nikolaos Stergioulas, and Deirdre Shoemaker. Observing Gravitational Waves From The Post-Merger Phase Of Binary Neutron Star Coalescence. *Class. Quant. Grav.*, 33(8):085003, 2016.

[6] Marcella Wijngaarden, Katerina Chatziioannou, Andreas Bauswein, James A. Clark, and Neil J. Cornish. Probing neutron stars with the full premerger and postmerger gravitational wave signal from binary coalescences. *Phys. Rev. D*, 105(10):104019, 2022.

[7] Benjamin P Abbott et al. A guide to LIGO–Virgo detector noise and extraction of transient gravitational-wave signals. *Class. Quant. Grav.*, 37(5):055002, 2020.